Non-uniform interpolatory subdivision via splines

Kęstutis Karčiauskas[a] and Jörg Peters[b]
[a] Vilnius University [b] University of Florida

Abstract

We present a framework for deriving non-uniform interpolatory subdivision algorithms closely related to non-uniform spline interpolants. Families of symmetric non-uniform interpolatory $2n$-point schemes of smoothness C^{n-1} are presented for $n = 2, 3, 4$ and even higher order, as well as a variety of non-uniform 6-point schemes with C^3 continuity.

1. Introduction

Uniform linear curve subdivision is well understood (see e.g. [DL02, Sab10]) but is too restrictive for some applications. One approach to enriching the shape repertoire of subdivision curves is to devise non-linear or geometric schemes such as [ADS10], [DH]. We, instead, focus on subdivision that starts with non-uniformly-spaced abscissae, e.g. spaced according to the distance between interpolated data points. Motivated by the fact that interpolatory 4-point subdivision [DLG88] can be interpreted as (up)sampling a C^1 Catmull-Rom spline, we extend the idea by devising a number of non-uniform interpolating splines and then filter out those combinations of interpolant values and control points that yield C^k schemes. The unexpectedly simple characteristic polynomials of the new Catmull-Rom-based C^1 and C^2 subdivision schemes enables us to fully analyze their continuity. For higher-order schemes, analysis via Rouche's theorem and separation of roots allow for symbolically filtering out new schemes of remarkably high smoothness.

1.1. Literature

Interpolatory subdivision algorithms with non-uniform parameter spacing or knots were analyzed by Warren [War95] and generalized in [DGS99]. Warren's constructions associate new points with the midpoints of knot-intervals and so create internally uniformly partitioned segments that join non-uniformly at extraordinary points. The corresponding continuity analysis can then focus on the extraordinary points and uses spectral analysis, well-known in the context of surfaces [DS78, WW02, PR08], but here applied to interpolatory curve subdivision. We build on Warren's approach but apply additionally Rouché's Theorem [Lan85] to recast the otherwise difficult estimates suitable for symbolic computing. Compared to [War95, DGS99] our schemes are simpler or yield higher continuity: neither Warren nor Daubechies achieve C^3 for 6-point schemes.

Our linear, non-uniform, interpolatory subdivision constructions are similar in spirit to those of [BCR11a, BCR11b] but differ in the detail. For example, in [BCR11b] one up-samples fundamental splines with non-uniform knots (NULIFS). We use and create different families of spline interpolants, e.g. a parameterized form of the non-uniform Catmull-Rom spline for the C^1 rule and its generalization for a non-uniform C^2 6-point construction. Low degree spline constructions even yield C^3 non-uniform 6-point schemes, and higher-order schemes can be derived by similar recipes. Both [BCR11a, BCR11b] have degrees of freedom associated with edges, while our constructions focus on a global parameter w familiar from the classic 4-point scheme [DLG88] and the 6-point Weissman scheme [Wei90].

Overview. We use results in the literature and the z-transform to establish smoothness in the uniform case, then analyze non-uniform subdivision similar to [War95]. Symbolic computation is essential for otherwise tedious book-keeping during the analysis. We do not attempt to typeset the intermediate expressions but rather present the framework of proof. For all examples, we use knot-sequences with centripetal spacing. We do not modify shape by adjusting knot-spacing, noting that, in the case of splines, shape is better controlled by adjusting local tension parameters.

Section 2 reviews basic techniques of non-uniform, geometric spline theory for use in the interpolants and introduces the local polynomial interpolants and splines to be sampled for our constructions. Section 3 reviews the known uniform interpolatory subdivision schemes and presents the analysis-framework for non-uniform, symmetric, interpolatory binary $2n$-point subdivision. Section 4 defines and analyzes new 4-point, 6-point and higher-order subdivision schemes. Section 5 briefly compares the new subdivision schemes to the underlying splines.

2. Non-uniform interpolatory splines

Since we will sample splines to obtain new points, we briefly recall some facts about interpolatory splines in Bézier form. We then introduce specialized spline constructions for our sampling.

2.1. Splines and jets in Bézier form

We refer to two curve segments f and g, each defined over the unit interval $[0\,..\,1]$, as C^r connected at common point $g(0) = f(1)$ if

$$g^{(k)}(0) = \beta^k f^{(k)}(1),\ k = 1, \ldots, r. \tag{1}$$

This is a special case of G^r continuity with linear reparameterization. Let $\{t_i\}$ be a sequence of strictly increasing numbers, called knots. We set β for the ith join of segments at t_i to

$$\beta_i := \frac{t_{i+1} - t_i}{t_i - t_{i-1}}, \tag{2}$$

mimicking the transitions of non-uniform C^r splines with interval ratio β_i at t_i. Then the *linear* reparameterization $t \to t_i(1-t) + t_{i+1}t$ turns segments related by (1) into standard C^r splines with knot sequence $\{t_i\}$. Conversely, the linear reparameterization

$t \to \frac{t-t_i}{t_{i+1}-t_i}$ relates splines to segments related by (1). To emphasize this special relation, we refer to the curve segments satisfying (1) as C^r connected rather than G^r connected. If $f(t) := \sum_{j=0}^{m} \tilde{\mathbf{b}}_j B_j(t)$ and $g(t) := \sum_{j=0}^{m} \mathbf{b}_j B_j(t)$ are in Bézier form, i.e. $B_j(t) := \binom{m}{j}(1-t)^{m-j}t^j$, then f and g join

C^0 if $\mathbf{b}_0 := \tilde{\mathbf{b}}_m$;

C^1 if they join C^0 and

$$\mathbf{b}_0 := \frac{\beta}{1+\beta}\tilde{\mathbf{b}}_{m-1} + \frac{1}{1+\beta}\mathbf{b}_1; \tag{3}$$

C^2 if they join C^0 and

$$\mathbf{b}_1 := a_0\tilde{\mathbf{b}}_{m-2} + a_1\mathbf{b}_0 + a_2\mathbf{b}_2, \quad \tilde{\mathbf{b}}_{m-1} := \tilde{a}_0\tilde{\mathbf{b}}_{m-2} + \tilde{a}_1\mathbf{b}_0 + \tilde{a}_2\mathbf{b}_2, \tag{4}$$
$$a_0 := -\frac{\beta^2}{2(1+\beta)},\ a_1 := \frac{1+\beta}{2},\ a_2 := \frac{1}{2(1+\beta)};$$

C^3 if they join C^1 and

$$\mathbf{b}_2 := a_0\tilde{\mathbf{b}}_{m-3} + a_1\tilde{\mathbf{b}}_{m-1} + a_2\mathbf{b}_1 + a_3\mathbf{b}_3, \tag{5}$$
$$\tilde{\mathbf{b}}_{m-2} := \tilde{a}_0\tilde{\mathbf{b}}_{m-3} + \tilde{a}_1\tilde{\mathbf{b}}_{m-1} + \tilde{a}_2\mathbf{b}_1 + \tilde{a}_3\mathbf{b}_3,$$
$$a_0 := \frac{\beta^3}{3(1+\beta)},\ a_1 := -\frac{1}{3}\beta(1+\beta),\ a_2 := \frac{2}{3}(1+\beta),\ a_3 := \frac{1}{3(1+\beta)}$$

where, for C^r continuity, $\tilde{a}_k$ is defined by replacing $\beta \to \frac{1}{\beta}$ in a_{r-k}.

Since C^r continuity involves only the first or the last $r+1$ Bézier coefficients of either curve, we define *local r-jets* at either endpoint of a degree m Bézier curve g as

$$\mathbf{J}_0^{r,m}(g) := \{\mathbf{b}_i\}_{i=0,\ldots,r}, \quad \mathbf{J}_1^{r,m}(g) := \{\mathbf{b}_i^* := \mathbf{b}_{m-i}\}_{i=0,\ldots,r}. \tag{6}$$

Since neither re-representing the r-jets in degree-k form for $k \neq m$, $k \geq r$, nor change of variable affect C^r-continuity, we freely use representations of a jet in different degree form or after change of variable and drop the second superscript m of $\mathbf{J}_i^{r,m}$. Specifically, $\mathbf{J}_i^{r,m}$ can be represented as $\mathbf{J}_i^{r,n}$ in terms of the coefficients $\hat{\mathbf{b}}_j$ of the curve of degree n, $n \geq r$, where $\hat{\mathbf{b}}_0 := \mathbf{b}_0$ and for $i = 1, \ldots, r; j = 0, \ldots, i$:

$$\hat{\mathbf{b}}_i := \sum_{j=0}^{i} c_{ij}^{mn}\mathbf{b}_j,\ c_{ij}^{mn} := \binom{i}{j}\frac{\prod_{s=0}^{j-1}(m-s)\prod_{s=0}^{i-j-1}(n-m-s)}{\prod_{s=0}^{i-1}(n-s)}. \tag{7}$$

After the change of variable $u \to \sigma u$, the new jet-points $\dot{\mathbf{b}}_i$ are defined by formula

$$\dot{\mathbf{b}}_i := \sum_{s=0}^{i}\binom{i}{s}(1-\sigma)^{i-s}\sigma^s\mathbf{b}_s. \tag{8}$$

If $\mathbf{J}_1^r(f)$ is scaled by σ^{left} and $\mathbf{J}_0^r(g)$ by σ^{right}, then the original parameter β is replaced by $\frac{\sigma^{right}}{\sigma^{left}}\beta$.

The coefficients of two C^r jets can be concatenated into the $2r+2$ tuple $\{\mathbf{b}_0, \ldots, \mathbf{b}_r, \mathbf{b}_r^*, \ldots, \mathbf{b}_0^*\}$ that can be interpreted as the coefficients of a Bézier curve of

degree $2r+1$. Alternatively, after scaling the variable by $\sigma := 1/(r+1)$ and adjusting the degree, the jets can be interpolated by a C^r-spline consisting of $r+1$ pieces of degree $r+1$. We use both constructions to generate families of spline interpolants from which samples are derived for interpolatory subdivision.

2.2. Polynomial interpolants, Catmull-Rom splines and their descendants

Let $\mathbf{f}_i^k$ be the polynomial of degree k that interpolates, for $s = 0, \ldots, k$, the points $\mathbf{p}_{i-\kappa+s}$ at the values $t_{i-\kappa+s}$ where $\kappa := \lfloor \frac{k}{2} \rfloor$. We define the localized interpolant to be (see Fig. 1a):

$$\bar{\mathbf{f}}_{i,j}^k(u) := \mathbf{f}_j^k((1-u)t_i + ut_{i+1}),\ u \in [0\,..\,1]. \tag{9}$$

C^1 splines. We represent the C^1-jets $\mathbf{J}_0^1(\bar{\mathbf{f}}_{i,i}^2)$ and $\mathbf{J}_1^1(\bar{\mathbf{f}}_{i,i+1}^2)$, in degree 3 form and concatenate them to form a cubic interpolant of $\mathbf{p}_i$ and $\mathbf{p}_{i+1}$. Since we can scale the variable and hence the tangent by ω, we denote this spline by cr_ω^1. That is, with b_i the control points of the classic Catmull-Rom spline cr_1^1 (Fig. 1b, top), cr_ω^1 has the same endpoints but interior coefficients $(1-\omega)\mathbf{b}_0 + \omega\mathbf{b}_1$ and $(1-\omega)\mathbf{b}_3 + \omega\mathbf{b}_2$.

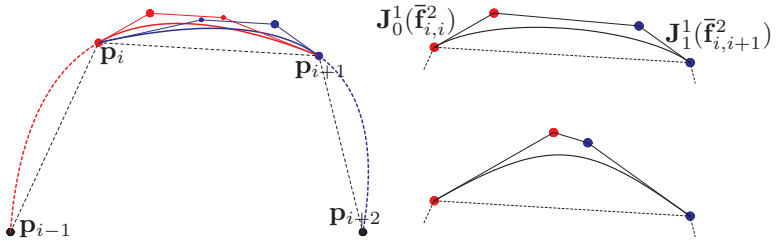

(a) Local interpolants (b) ω-scaling

Figure 1: Construction of Catmull-Rom splines. (a) The left (red) interpolant $\mathbf{f}_i^2$ and its localization $\bar{\mathbf{f}}_{i,i}^2$ provide the left two Bézier coefficients, collected in $\mathbf{J}_0^1(\bar{\mathbf{f}}_{i,i}^2)$, of the cubic cr_1^1 (disks in (b), top). Concatenation with the right (blue) jet $\mathbf{J}_1^1(\bar{\mathbf{f}}_{i,i+1}^2)$ yields all four coefficients of cr_1^1. (b) *bottom* illustrates cr_2^1, i.e. scaling by 2.

From cr_ω^1, we can derive piecewise quadratic C^1 splines as follows. We represent the C^1-jets $\mathbf{J}_0^1(f_i)$ and $\mathbf{J}_1^1(f_i)$ of the cubic segment f_i in degree 2 form and scale the variable by $\frac{1}{2}$. Then choosing the common point of the two quadratics to be $f_i(\frac{1}{2})$ yields a C^1 join between the pieces! We denote this spline by $\mathrm{cr}_\omega^{1,2}$. The spline $\mathrm{cr}_1^{1,2}$ ($\omega = 1$) coincides with the symmetric C^1 quadratic NULIFS used in [BCR11b].

C^2 splines. We re-represent the ith segment of cr_ω^1, f_i, in degree 4 form with control points $\mathbf{b}_k^i$, $k = 0, \ldots, 4$ and then redefine $\mathbf{b}_1^i$, $\mathbf{b}_3^i$ according to (4). This yields the spline cr_ω^2. The same construction, starting with $\bar{\mathbf{f}}_{i,i}^3(u)$ in place of cr_ω^1, yields the spline $\mathrm{cu}^{2,4}$.

In turn, each degree 4 segment can be replaced by two C^2-connected cubics. This yields the splines denoted as $\mathrm{cr}_\omega^{2,3}$ and $\mathrm{cu}^{2,3}$. The splines $\mathrm{cu}^{2,3}$ coincide with symmetric C^2 cubic NULIFS. In more detail, the two C^2-connected cubics interpolate the quartic's C^2-jets $\mathbf{J}_0^2(f)$ and $\mathbf{J}_1^2(f)$ – in degree 3 form and with the variable scaled by $\frac{1}{2}$ –

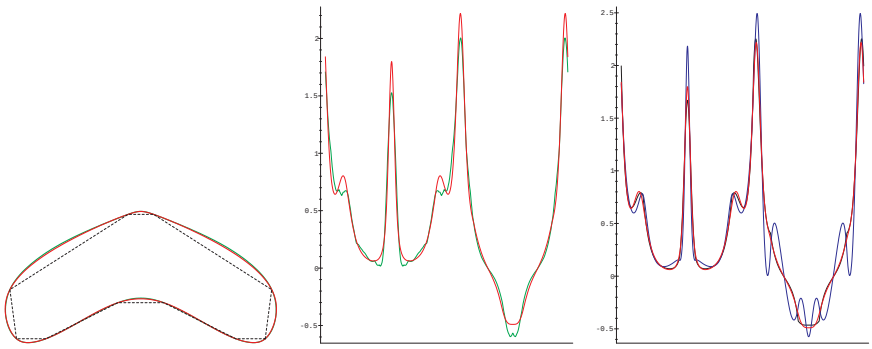

(a) Polygon and curves (b) curvatures (c) direct smoothing

Figure 2: C^3 curves. red: C^3 spline from $\mathrm{cr}^2_{1.15}$; green: 6-point $\mathrm{A}^{3,5:3:3}_{0.0141}$-subdivision; blue: C^3 spline directly from $\mathrm{cr}^1_{1.15}$.

and share the common point

$$\mathbf{m}^4(f) := \frac{1}{12}(\mathbf{b}_0 + \mathbf{b}_4) + \frac{1}{6}(\mathbf{b}_1 + \mathbf{b}_3) + \frac{1}{2}\mathbf{b}_2. \tag{10}$$

Remarkably, the so-constructed cubics join C^2. (The analoguous construction for degree 5 curves would only join C^1.)

Repeated smoothing of interpolating splines. To derive interpolating splines of higher continuity from those of lower, we interlace degree-raising with smoothing corrections (3), (4), (5), etc. Compared to immediately setting the degree and enforcing smoothness, this step-by-step procedure yields, over many trials, better curvature distribution, as illustrated in Fig. 2b,c. For example, we get $\mathrm{cr}^2_{1.15}$ from $\mathrm{cr}^1_{1.15}$ via degree-raising followed by (4) and then increase smoothness from C^2 to C^3 by degree-raising to 6 with Bézier coefficients $\mathbf{b}^i_k$, $k = 0, \ldots, 6$ and finally overwriting $\mathbf{b}^i_2$ and $\mathbf{b}^{i-1}_4$ according to (5). If, instead, we immediately enforced C^3 continuity for degree-raised C^1 splines $\mathrm{cr}^1_{1.15}$, the curvature distribution is clearly worse Fig. 2c. We note that the degree of the spline can be reduced by replacing the single piece of degree 6 by four C^3-joined sub-segments of degree 4.

3. A framework for non-uniform interpolatory subdivision

Given a sequence of increasing scalars $\{t_i\}$, called knots, and a sequence of points $\{\mathbf{p}_i\}$ in $\mathbf{R}^d$, the $k+1$st point sequence is derived from the kth, starting with $\mathbf{p}^0_i := \mathbf{p}_i$, by

$$\mathbf{p}^{k+1}_{2i} := \mathbf{p}^k_i \ , \quad \mathbf{p}^{k+1}_{2i+1} := \sum_{j=1}^{2n} e_{ij}\mathbf{p}^k_{i-n+j}. \tag{11}$$

That is, in every refinement step, we insert one new point between two old ones. The $2n$ coefficients e_{ij} depend on $2n-2$ scalars $\beta_{i-n+2}, \ldots, \beta_{i+n-1}$ that in turn depend on the

Table 1: Uniform symmetric C^{n-1} $2n$-point interpolatory schemes with parameter w.

$2n$	$\bar{e}_j, j = 1, \ldots, n$	C^{n-1} range for w
4	$-w, w + \frac{1}{2}$	[HMR09]
6	$w, -3w - \frac{1}{16}, 2w + \frac{9}{16}$	$(0\,..\,0.042]$
8	$-w, 5w + \frac{3}{256}, -9w - \frac{25}{256}, 5w + \frac{75}{128}$;	$[0.0016\,..\,0.0084]$
10	$w, -7w - \frac{5}{2048}, 20w + \frac{49}{2048}, -28w - \frac{245}{2048}, 14w + \frac{1225}{2048}$	$[0.0005\,..\,0.0016]$

knots via $\beta_i := \frac{t_{i+1}-t_i}{t_i-t_{i-1}}$, the ratio of the adjacent knot intervals. In our constructions, new knots are picked as midpoints of intervals $t^{k+1}_{2i+1} := \frac{1}{2}(t^k_i + t^k_{i+1}), t^{k+1}_{2i} := t^k_i$, a choice that [DGS99] calls semi-regular. Therefore

$$\beta^{k+1}_{2i} := \beta^k_i, \quad \beta^{k+1}_{2i+1} := 1. \tag{12}$$

All constructions will be invariant under the replacements

symmetry: $e_{ij} \to e_{i,2n+1-j}$ $\beta_{i-n+2+s} \to (\beta_{i+n-1-s})^{-1}$,

translation: $e_{ij} \to e_{i+s,j}$ $\beta_{i-n+2}, \ldots, \beta_{i+n-1} \to \beta_{i-n+2+s}, \ldots, \beta_{i+n-1+s}$.

Following [War95], we first establish the smoothness in the uniform case $\beta_i = 1$. Then we focus on the isolated extraordinary points corresponding to an isolated $\beta \neq 1$.

3.1. Review of uniform symmetric $2n$-point interpolatory schemes with parameter w

For uniform knots $\beta_i = 1$ for all i. Abbreviating the coefficients to $\bar{e}_j$, we obtain the Laurent polynomial $a(z) := \sum_{j=1}^{n} \bar{e}_j z^{-2n-1+2j} + 1 + \sum_{j=n+1}^{2n} \bar{e}_j z^{-2n-1+2j}$. For the schemes in this paper,

$$a(z) = \frac{(1+z)^{m+1}}{2^m} b(z), \tag{13}$$

i.e. the schemes are C^m if for some integer $l > 0$ $||S^{[l]}_b||_\infty < 1$, where $S^{[l]}_b := \max\left\{\sum_{j\in\mathbf{Z}} |b^{[l]}_{i-2^l j}| : 0 \leq i < 2^l, b^{[l]}(z) := b(z)b(z^2)\cdots b(z^{2^{l-1}})\right\}$ [Dyn92, DL02, DFH04]. Table 1 lists the classical 4-point scheme and its generalizations, such as Weissman's 6-point and higher-order schemes from [KLY07] (with correction of the 8-point scheme). Since $\bar{e}_{2n-i} = \bar{e}_i$, Table 1 only lists $\bar{e}_j$, $j = 1, \ldots, n$. The maximal range for w for the 4-point scheme was derived in [HMR09].

3.2. Framework for proving C^m continuity of non-uniform symmetric interpolatory $2n$-point subdivision

Following [War95], the now isolated non-uniform locations can be analyzed by the following process. This process typically benefits from symbolic computation to avoid tedious book-keeping and consists of the following four steps.

1. Repeated knot insertion at the middle of intervals isolates each knot where $\beta \neq 1$ by surrounding it by knots where $\beta = 1$. The β at this isolated extraordinary knot is denoted γ in the following.

2. Uniform subdivision applies where $\beta = 1$. Table 1 gives the w-ranges for C^m continuity.

3. The $(4n-1) \times (4n-1)$ subdivision matrix L for the now isolated extraordinary point has the rows

$$\begin{aligned} L_1 &:= (E_0, \mathbf{0}^{2n-1}); \quad L_{4n-1} := (\mathbf{0}^{2n-1}, E_0); \\ L_{2i} &:= (\mathbf{0}^{n-1+i}, 1, \mathbf{0}^{3n-1-i}) \ , \ i = 1, \ldots, 2n-1, \\ L_{2i+1} &:= (\mathbf{0}^{i}, E_i, \mathbf{0}^{2n-1-i}) \ , \ i = 1, \ldots, 2n-2, \end{aligned} \tag{14}$$

   where $\mathbf{0}^s$ is a sequence of s zeros,

$$E(\beta_{i-n+2}, \ldots \beta_{i+n-1}) := (e_{i1}, \ldots, e_{i,2n}),$$

   maps the $2n-2$ ratios β to the $2n$ coefficients e_{ij}, and, with $\mathbf{1}^s$ a sequence of s ones, $E_k := E(\mathbf{1}^{2n-2-k}, \gamma, \mathbf{1}^{k-1})$, $k = 1, \ldots, 2n-2$, $E_0 := E(\mathbf{1}^{2n-2})$. For an example see e.g. [War95, Sec.5].

   Since the constructions are chosen to reproduce polynomials up to degree m, the matrix L has eigenvalues $1, \frac{1}{2}, \ldots, \frac{1}{2^m}$ whose eigenfunctions are the polynomials $1, t, \ldots, t^m$. The characteristic polynomial $\chi(\lambda)$ of L is

$$\chi(\lambda) = const(\lambda - 1)(\lambda - \frac{1}{2}) \cdots (\lambda - \frac{1}{2^m})\ell(\lambda)r(\lambda), \tag{15}$$

   where the roots of the polynomial $\ell(\lambda)$ are *dominated* by $\frac{1}{2^m}$, i.e. absolute value of the roots is strictly less than $\frac{1}{2^m}$.

4. It only remains to prove that the roots of the polynomial $r(\lambda)$ are dominated by $\hat{\lambda} := \frac{1}{2^m}$. We note that $r(\lambda)$ also depends on the extraordinary ratio γ.

   a. Let $\tilde{r}(\lambda)$ be the polynomial obtained by replacing $\gamma \to \frac{1}{\gamma}$. By checking that $\tilde{r}(\lambda)\gamma^{\tilde{m}} = r(\lambda)$ for some $\tilde{m}$, we may assume that $\gamma \in (0, 1]$.

   b. Since we only want to show C^m continuity for some range of the parameter w, we select a candidate range $[\underline{w}, \overline{w}]$ by experiment. (Maximal bounds can be hard to determine; see [HMR09]).

   c. $r(\lambda) := \sum_{s=0}^{p} d_s(\gamma, w)\lambda^s$ has coefficients $d_s(\gamma, w)$ that are themselves polynomials (with Bézier coefficients d_{ij}^s) of bi-degree $k' \times k''$ over $[0, 1] \times [\underline{w}, \overline{w}]$.

   d. We check, for each pair (i, j) separately, by symbolic computation that

$$\sum_{s=0}^{p-1} |d_{ij}^s| \hat{\lambda}^s - d_{ij}^p \hat{\lambda}^p < 0, \quad d_{ij}^p > 0 \ . \tag{16}$$

   Let $g(z) := \sum_{s=0}^{p} d_s(\gamma, w) z^s$ and $h(z) := d_p(\gamma, w) z^p$ for z on a circle of radius $\hat{\lambda}$. Then (16) implies the strict inequality in

$$|g(z) - h(z)| = |\sum_{s=0}^{p-1} d_s z^s| \leq \sum_{s=0}^{p-1} |d_s||z^s| < |h(z)|.$$

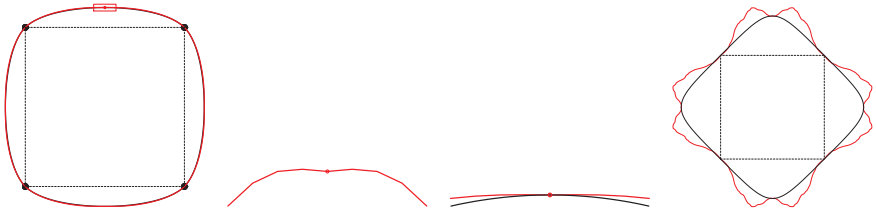

(a) default $w = \frac{1}{16}$ (b) scaled magnification (c) flatness (d) extreme $w = 0.19$

Figure 3: Comparing, for an input square, (a) 4-point subdivision (with default $w = 1/16$, red, to the Catmull-Rom spline, black. (b) Magnification, vertically scaled by 50, after six subdivision steps, (c) magnification near a first-inserted point, without vertical scaling. Changing the parameter w to its extreme value results in an almost fractal 4-point curve but a reasonable Catmull-Rom variant (see (1)).

Rouché's Theorem [Lan85] implies that g and h have the same number p of roots in the $\hat{\lambda}$-disk, i.e. by the degree of g all roots of g are confined to the $\hat{\lambda}$-disk and hence $r(\lambda)$ is dominated by $\hat{\lambda} := \frac{1}{2^m}$.

With this framework, proving smoothness of a new scheme requires only determining ℓ and r, and verifying that their roots are dominated by $\frac{1}{2^m}$.

4. Non-uniform interpolatory subdivision

We concretely determine formula (11) for the new point $\tilde{\mathbf{p}}_{2i+1}$ by combining values of local interpolants and their Bézier coefficients. We note that the rules below have been filtered from a large set of 'natural choices' using splines or Lagrange constructions. Many choices fail already as uniform rules or have the wrong spectrum or simply can not be analyzed by the presented techniques.

While it is customary to present the coefficients e_{ij} for each scheme, typesetting them for higher degree does not add insight. We therefore only present some formulas for lower degree, e.g. (17) and (19), to give the flavor. All formulas for e_{ij} can be generated by writing the interpolants in terms of t_i or in terms of β_i. We explicitly name only two families of subdivision schemes: CR_w^k and $\mathrm{A}_w^{k,\alpha}$. In either case the superscript k indicates the smoothness and α is a tuple specifying the degrees of sampled interpolants combined in the rule. CR is to remind of Catmull-Rom and A of averaging interpolants.

4.1. Non-uniform C^1 4-point subdivision rules

We define a new point $\mathbf{p}_{2i+1}^{k+1}$ of the scheme CR_w^1 by evaluating the segment of cr_{16w}^1 that joins the points $\mathbf{p}_i^k$ and $\mathbf{p}_{i+1}^k$. For uniform knots, i.e. $\beta = 1$, this new scheme reduces to the classic 4-point scheme. Equivalently, we can evaluate

$$\omega \frac{\bar{\mathbf{f}}_{i,i}^2(u) + \bar{\mathbf{f}}_{i,i+1}^2(u)}{2} + (1-\omega)\bar{\mathbf{f}}_{i,i}^1(u), \quad \omega = 16w,$$

(which proves that refinement rules preserve linear functions). The explicit rules are

$$e_{i1} := -2\frac{\beta_i^2}{1+\beta_i}w, \quad e_{i2} := \frac{1+\beta_{i+1}+4(\beta_i+\beta_i\beta_{i+1}-1)w}{2(1+\beta_{i+1})} \tag{17}$$

and the coefficients e_{i3}, e_{i4} are defined by symmetry (see definition after (12)). [HMR09] provides the exact range $(0\,..\,w^*)$ such that uniform 4-point subdivision with parameter $w \in (0\,..\,w^*)$ is C^1: $w^* \approx 0.19273$ is the unique real solution of the cubic equation $32w^3 + 4w - 1 = 0$.

Proposition 1. CR^1_w *subdivision is* C^1 *for the maximal range* $w \in (0\,..\,w^*)$.

The analysis of CR^1_w yields $\ell(\lambda) = (\lambda + w)^2(\lambda - 2w)$, $r(\lambda) = 2\lambda^2 - \lambda + 2w$. For w in the range defined by [HMR09], the roots of $r(\lambda)$ are dominated by $\frac{1}{2}$. |||
By contrast, defining the new point of a scheme by evaluating a combination of cubic and linear interpolants, $\mathrm{A}^{1,3:1}_w$ averaging,

$$\omega \bar{\mathbf{f}}^3_{i,i}(u) + (1-\omega)\bar{\mathbf{f}}^1_{i,i}(u), \quad \omega = 16w, \tag{18}$$

as in [Dyn92], does not allow for the full range of [HMR09]: for example, for $w := 0.13$, curves are generally not C^1.

4.2. Non-uniform C^2 6-point subdivision rules

In this section, we present four alternative non-uniform C^2 6-point subdivision rules: Repeated 4-point subdivision, CR^2_w subdivision, subdivision from $\mathrm{cu}^{2,4}$-splines and $\mathrm{A}^{2,5:3}_w$ subdivision. In each, the new point $\tilde{\mathbf{p}}_{2i+1}$ is defined by a knot sequence $\{t_{i-2+s}\}_{s=0,\ldots,5}$ and a point sequence $\{\mathbf{p}_{i-2+s}\}_{s=0,\ldots,5}$.

Repeated 4-point rule. We first create intermediate points $\hat{\mathbf{p}}_{2i+1}$ ($\hat{\mathbf{p}}_{2i} := \mathbf{p}_i$). The points $\hat{\mathbf{p}}_{2i+1}$ are computed from $\{\mathbf{p}_j\}_{i-1,i,i+1,i+2}$ by a 4-point scheme, either $\mathrm{CR}^1_{1/16}$ or $\mathrm{A}^{1,3:1}_{1/16}$ of (18). In a second step, we obtain $\tilde{\mathbf{p}}_{2i+1}$ by applying the same rule with scalars $2\beta_i$ and $\frac{1}{2}\beta_{i+1}$ to $\{\hat{\mathbf{p}}_j\}_{2i-1,2i,2i+2,2i+3}$ ($\tilde{\mathbf{p}}_{2i} := \mathbf{p}_i$). In the case of uniform spacing, this is the Weissman 6-point scheme with $w = 1/96$.

Proposition 2. *Repeated 4-point subdivision is* C^2.

For the $\mathrm{CR}^1_{1/16}$ scheme, $\ell(\lambda) = (\lambda - \frac{1}{96})^2$ and $r(\lambda, \gamma)$ is a polynomial of bi-degree $(s, 2)$ for $s = 6$. For the $\mathrm{A}^{1,3:1}_{1/16}$ scheme, $\ell(\lambda) = (\lambda - \frac{1}{8})(\lambda - \frac{1}{96})^2$ and $r(\lambda, \gamma)$ a polynomial of bi-degree $(s, 4)$ for $s = 5$. All roots of $r(\lambda)$ are real and dominated by $\frac{1}{4}$ since for an increasing sequence $\lambda_k \in [-\frac{1}{4}\,..\,\frac{1}{4}]$, $k = 0, \ldots s$, the sign of $r(\lambda_k, \cdot)$ alternates. |||

Despite its provenance, curvature plots of the scheme do not show severe problems; but, the curvature distribution of this construction is noisier than that of the following schemes.

Subdivision CR^2_w *from* cr^2_1 *splines.* The new point is defined by evaluating a segment f^i of cr^2_1 from $\mathbf{p}^k_i$ to $\mathbf{p}^k_{i+1}$ and averaging with the point $\mathbf{m}^4(f^i)$ of (10)

$$\tilde{\mathbf{p}}_{2i+1} := \tilde{\omega} f^i\big(\frac{1}{2}\big) + (1-\tilde{\omega})\mathbf{m}^4(f^i), \quad \tilde{\omega} := 576w - 2\,. \tag{19}$$

For $\omega = 1$, cr^2_ω reproduces quadratic polynomials. With the abbreviations $\beta_- := \beta_{i-1}$, $\beta := \beta_i$, $\beta_+ := \beta_{i+1}$, the explicit refinement rules are

$$e_{i1} := \frac{4\beta_-^2\beta^2}{(1+\beta_-)(1+\beta)}w,\ e_{i2} := -\frac{\beta^2(1+\beta_+ + 32(\beta_- + \beta_+ + \beta_-\beta_+)w)}{8(1+\beta)(1+\beta_+)},$$
$$e_{i3} := \frac{3+4\beta+4\beta_+ + 5\beta\beta_+ + 32w(\beta\beta_+ - 1)}{8(1+\beta)(1+\beta_+)} - e_{i1} - e_{i2},$$

and the coefficients e_{i4}, e_{i5}, e_{i6} are defined symmetrically. For a uniform knot sequence the scheme reduces to Weissman's 6-point subdivision [Wei90].

Proposition 3. CR^2_w *subdivision is* C^2.

The analysis yields $\ell(\lambda) = (\lambda - \frac{1}{8})(\lambda - w)^2$ and

$$r(\lambda) = \big(16\lambda^2 + (1-32w)\lambda - 256w^2\big)\big(64\lambda^3 + (256w-12)\lambda^2 + (64w-1)\lambda + 256w^2\big),$$

whose roots are dominated by $\frac{1}{4}$ when w is in the C^2-range of Table 1 for the uniform 6-point scheme. |||

The CR^2_w scheme is special in that its characteristic polynomial does not depend on the interval ratio γ. This simplifies the analysis compared to other C^2 6-point schemes discussed next.

Subdivision from $\mathrm{cu}^{2,4}$ *splines.* Rules (19) applied to a segment of $\mathrm{cu}^{2,4}$ yields a C^2 6-point scheme that, for $w = \frac{1}{288}$, coincides with the symmetric version of the 6-point scheme in [BCR11b].

The $\mathrm{A}^{2,5:3}_w$ *6-point* C^2 *scheme.* Averaging values of a quintic and a cubic interpolant defines new points of the $\mathrm{A}^{2,5:3}_w$ as

$$\tilde{\mathbf{p}}_{2i+1} := \omega\bar{\mathbf{f}}^5_{i,i}(\frac{1}{2}) + (1-\omega)\bar{\mathbf{f}}^3_{i,i}(\frac{1}{2}), \quad \omega := \frac{256}{3}w. \tag{20}$$

For $w := \frac{3}{256}$, $\mathrm{A}^{2,5:3}_w$ coincides with the scheme investigated in [War95].

Proposition 4. $\mathrm{A}^{2,5:3}_w$ *subdivision is* C^2.

The analysis yields $\ell(\lambda) = (\lambda - \frac{1}{8})(\lambda - w)^2$, and $r(\lambda)$ is a polynomial of degree 5 whose roots are dominated by $\frac{1}{4}$ when $w \in [0.001, 0.02]$ – which is a sub-range of the C^2-range of the uniform 6-point scheme (cf. Table 1). |||
Since $\mathrm{A}^{2,5:3}_w$ reproduces cubics, $\ell(\lambda)$ contains the factor $\lambda - \frac{1}{8}$ and a necessary condition for a uniform 6-point scheme to be C^3 is $0.0124 < w < 0.0169$ [Wei90]. However, close analysis for $\gamma \in (0, \frac{1}{10}]$ and w in the Weissman-range shows $r(\frac{1}{8}) < 0$ while $r(\frac{1}{2}) > 0$, implying that $r(\lambda)$ has a root greater than $\frac{1}{8}$.

4.3. Non-uniform C^3 *6-point subdivision rules*

Remarkably, two additional 6-point schemes can be shown to be C^3 for specific values of w. The new points of $\mathrm{A}^{3,5:3:3}_w$ subdivision are defined by

$$\tilde{\mathbf{p}}_{2i+1} := \omega\bar{\mathbf{f}}^5_{i,i}(\frac{1}{2}) + (1-\omega)\frac{1}{2}(\bar{\mathbf{f}}^3_{i,i-1}(\frac{1}{2}) + \bar{\mathbf{f}}^3_{i,i+1}(\frac{1}{2})), \quad \omega := \frac{8}{5} - \frac{256}{5}w. \tag{21}$$

For uniform knot sequences this scheme reduces to Weissman's 6-point subdivision. For $w := 3/256$, it becomes the 6-point rule analyzed in [War95].

Proposition 5. $\mathrm{A}^{3,5:3:3}_{0.0141}$ *is* C^3 *continuous.*

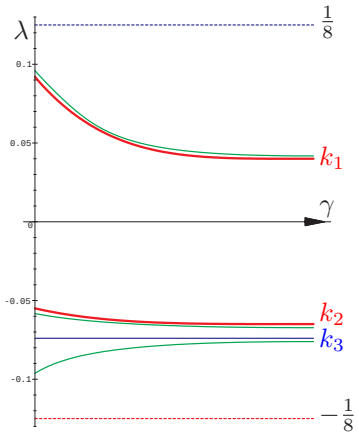

Figure 4: Bounding the roots of r as a function of λ and γ for $\mathrm{A}^{3,5:3:3}_{0.0141}$. The function r is positive when restricted to any blue curve and negative when restricted to red curves. The pre-images of $r = 0$ are green.

The characteristic polynomial has the factor $\lambda - \frac{1}{8}$ required for C^3 continuity, $\ell(\lambda) = (\lambda - w)^2$ and $r(\lambda)$ is a polynomial of degree 5. Since we only want to show the existence of a non-uniform C^3 6-point scheme, we check C^3 continuity for specific w values rather than for a range. Using the z-transform (13), the uniform Weissman scheme is found to be C^3 for $w = 0.0139, 0.0140, 0.0141, 0.0142, 0.0143$ since the norm $||S_b^{[l]}||_\infty < 1$ for $l = 9$. We chose the value $w = 0.0141$. The polynomial $r(\lambda)$ is of degree 5 in λ and of degree 8 in γ. (i) Since the coefficients of $r^+(u, \gamma) := r(\frac{1}{8} + u)$, $\gamma \in (0\,..\,1]$, are positive, the real roots of $r(\lambda)$ are less than $\frac{1}{8}$; and since the coefficients of $r^-(u, \gamma) := r(-\frac{1}{8} - u)$ are negative, the real roots of $r(\lambda)$ are greater than $-\frac{1}{8}$. That is, $r(\frac{1}{8}) > 0$ and $r(-\frac{1}{8}) < 0$. (ii) The two thick red curves $(\gamma, k_j(\gamma))$, $j = 1, 2$, in Fig. 4 are polynomials of degree 4. Restricting $r(\lambda)$ to the curves yields a polynomial of degree 28 in γ with all negative Bézier coefficients. (iii) The restriction of $r(\lambda)$ to $k_3 = -0.075$ has all positive Bézier coefficients. (iv) Hence, for any $\gamma \in (0\,..\,1]$, the polynomial $r(\lambda)$ of degree 5 has three (green) real root curves of modulus less than $\frac{1}{8}$. By (i), the remaining two roots must be complex-conjugate, if their modulus is greater or equal to $\frac{1}{8}$. Denoting the coefficients of $r(\lambda)$ by $a_k(\gamma)$, the complex-conjugate roots are bounded by $\sqrt{|a_0|/(|a_5||k_1||k_2||k_3|)} < \frac{1}{8}$, proving, by contradiction, that all roots of $r(\lambda)$ are modulo $< \frac{1}{8}$. |||

Alternatively, for f of degree 5 with coefficients $\mathbf{b}_i$, $i = 0, \ldots, 5$, we replace f by two C^1 connected cubics that match its scaled 2-jets and set their common point to

$$\mathbf{m}^5(f) := \frac{1}{12}(\mathbf{b}_0 + \mathbf{b}_5) + \frac{5}{12}(\mathbf{b}_2 + \mathbf{b}_3)$$

(which coincides with $f\big(\frac{1}{2}\big)$ if f is a degree-raised cubic). The new points of the scheme $\mathrm{A}^{3,5}_w$ are

$$\tilde{\mathbf{p}}_{2i+1} := \omega \bar{\mathbf{f}}^5_{i,i}\big(\frac{1}{2}\big) + (1 - \omega)\mathbf{m}^5(\bar{\mathbf{f}}^5_{i,i}),\ \omega := 28 - 2304w\,. \tag{22}$$

For $w := 0.0141$ the proof of C^3 continuity follows that for the $\mathrm{A}^{3,5:3:3}_{0.0141}$ scheme.

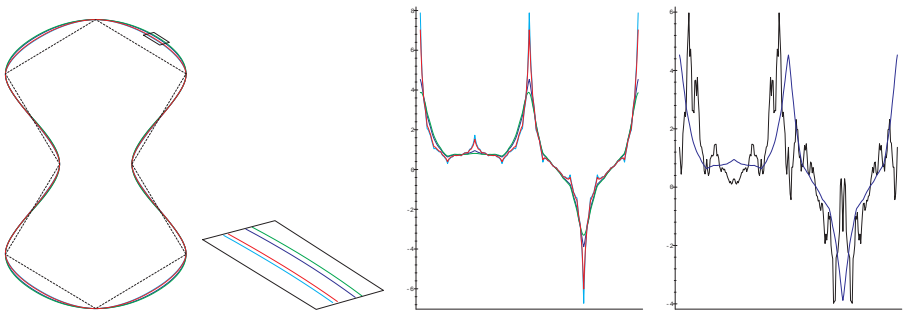

(a) Curves (b) magnification (c) 'normal' curvatures (d) extreme curvature

Figure 5: Uniform Weissman 6-point scheme for various w; green: $w := 0.0141$; blue: $w := \frac{3}{256}$; red: $w := \frac{1}{192}$; cyan: $w := \frac{1}{288}$; black: $w := 0.04$. Due to symmetry only a half of curvature plots are displayed.

Comparing 6-point schemes. Since much of each subdivision curve is defined by the uniform Weissman rules, we focus on setting the weight w for the uniform case. Fig. 5a shows an input polygon with sides of equal length. Smaller w yields a curve that more closely hugs the input polygon (cf. (b)) and shows a poorer curvature distribution, Fig. 5c. Weights as small as $w = 0.001$ make the $\mathrm{A}_w^{2,5:3}$-scheme very close to a classic 4-point scheme with $w = \frac{1}{16}$ and Fig. 5d demonstrates that the upper bound $w = 0.042$ of C^2-range of Table 1 is equally undesirable. Similar to the C^1 4-point scheme, we can therefore say that CR_w^2 realizes the full practical range of w.

4.4. Subdivision of higher continuity

We present here non-uniform C^3 8-point and C^4 10-point schemes, and a *uniform* C^5 12-point subdivision scheme. The C^5 12-point scheme does not appear in the literature, presumably because a uniform Deslauriers-Dubuc scheme from degree 11 interpolants is only C^4 [Rio92] (which implies that the conjecture in [War95], that interpolatory schemes with order $2r + 1$ polynomial precision are C^r continuous, is incorrect). The earlier 6-point constructions hinted that higher-order schemes are better derived by up-sampling the local interpolants rather than high-order splines.

Non-uniform C^3 8-point subdivision. New points are defined as

$$\tilde{\mathbf{p}}_{2i+1} := \omega \bar{\mathbf{f}}_{i,i}^7(\frac{1}{2}) + (1-\omega)\bar{\mathbf{f}}_{i,i}^5(\frac{1}{2}), \quad \omega := \frac{2048}{5}w. \tag{23}$$

For uniform knot sequence this scheme reduces to the 8-point scheme of [KLY07].

The analysis yields $\ell(\lambda) = (\lambda - \frac{1}{16})(\lambda - \frac{1}{32})(\lambda + w)^2$ and $r(\lambda)$ is a polynomial of degree 7 whose roots are dominated by $\frac{1}{8}$ when $w \in [0.0011, 0.0035]$; therefore the scheme is C^3.

Non-uniform C^4 10-point subdivision. New points are defined as

$$\tilde{\mathbf{p}}_{2i+1} := \omega \bar{\mathbf{f}}_{i,i}^7(\frac{1}{2}) + (1-\omega)\frac{1}{2}(\bar{\mathbf{f}}_{i,i-1}^7(\frac{1}{2}) + \bar{\mathbf{f}}_{i,i+1}^7(\frac{1}{2})), \quad \omega := 1 - \frac{4096}{5}w. \tag{24}$$

For uniform knot sequences this scheme reduces to a 10-point scheme of [KLY07].

The analysis yields $\ell(\lambda) = (\lambda - \frac{1}{32})(\lambda - \frac{1}{64})(\lambda - \frac{1}{128})(\lambda - w)^2$ and $r(\lambda)$ is a polynomial of degree 9 whose roots are dominated by $\frac{1}{16}$ when $w \in [0.000915, 0.001046]$. Therefore a scheme is C^4.

Uniform C^5 12-point subdivision. New points are defined as

$$\tilde{\mathbf{p}}_{2i+1} := \omega \bar{\mathbf{f}}^{11}_{i,i}(\frac{1}{2}) + (1-\omega)\bar{\mathbf{f}}^{9}_{i,i}(\frac{1}{2}), \quad \omega := 2. \tag{25}$$

Using the z-transform (13), we checked that the scheme is C^5 with norm $||S_b^{[l]}||_\infty < 1$ for $l = 7$.

5. Non-uniform schemes vs splines

The construction of subdivision schemes via splines raises the question 'why not use the spline directly'. After all, subdivision continuity analysis requires non-trivial spectral analysis while explicit formulas for smooth splines are comparatively easy to derive (see e.g. (5)).

Part of the answer is that the schemes ultimately feed into surface constructions, where extraordinary points present challenges regardless of whether spline or subdivision schemes are chosen. Another is that we do not fully understand the trade-off in terms of curvature distribution. Sometimes the localized, step-by-step subdivision construction performs better than splines, while usually splines have better global behavior since step-by-step procedures introduce higher frequencies. (A similar trade-off exists, but is not discussed here, when we add flexibility via tension parameters.)

As a first example, Fig. 3 juxtaposes 4-point subdivision [DLG88] and the Catmull-Rom spline [CR74]. Visually, in Fig. 3a, the two curves are barely distinguishable. However, while the classical 4-point scheme somewhat surprisingly does not even preserve the convexity of the input square (Fig. 3b), the simple spline remains convex. Conversely, 4-point subdivision is unduly flat near the first-inserted points Fig. 3c.

Fig. 6a shows that, visually, the cr_1^2 spline and the CR_1^2 subdivision are hard to distinguish. However (b) shows higher curvature fluctuation for the subdivision curve while (c) shows $\mathrm{A}^{2,5:3}$-subdivision improving on cr_1^2 splines. (We note that $\omega = 1$ is mandatory to obtain C^2 subdivision. The splines still have an option of changing ω. Experiments show that $\omega = 1.15$ is a better choice, not only for this configuration.) Fig. 7 provides a third comparison. In Fig. 7a only $\mathrm{cr}^2_{1.15}$ is displayed since the other curves are visually indistinguishable. Fig. 7b shows improved curvature distribution from the default $\mathrm{CR}^2_{1/192}$ to $\mathrm{CR}^2_{0.0141}$ and from $\mathrm{A}^{2,5:3}_{3/256}$ to $\mathrm{A}^{2,5:3}_{0.0141}$ – even though $\mathrm{A}^{2,5:3}_{3/256}$ reproduces up to degree 5 while $\mathrm{A}^{2,5:3}_{0.0141}$ reproduces polynomials only up to degree 3. While, for uniformly spaced data, increased degree of reproduction is usually associated with better shape, reduced degree appears better for strongly non-uniform configurations. Fig. 8 illustrates how higher reproduction capability derived from higher degree interpolants either has low fidelity to the input shape or results in worse shape for strongly non-uniform inputs. The simple T-input, inspired by [BCR11b], results in smooth curves that do not follow the initial shape closely. Replacing the corners

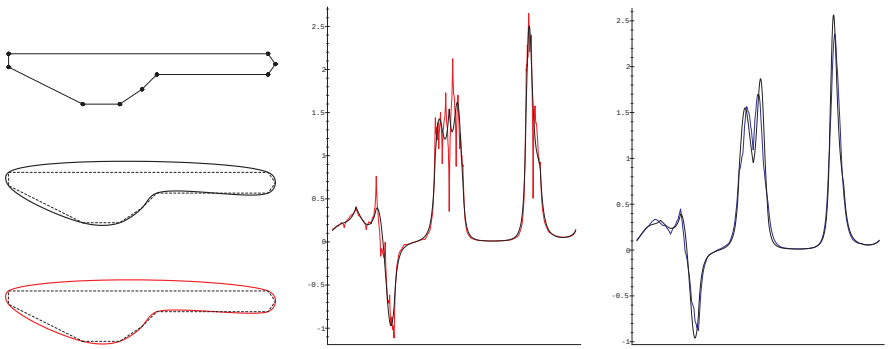

(a) Polygon and curves (b) cr_1^2; $\mathrm{CR}^2_{1/192}$ (c) $\mathrm{cr}^2_{1.15}$; $\mathrm{A}^{2,5:3}_{3/256}$

Figure 6: (a) (*top*) A polygon (from a talk by Nira Dyn), (*middle*) the interpolating spline cr_1^2 with original $\omega = 1$, (*bottom*) the corresponding CR^2_w subdivision with $w = \frac{1}{192}$. (b) Curvature plots of (a). (c) Curvature plots of: blue – $\mathrm{A}^{2,5:3}_{3/256}$; black – $\mathrm{cr}^2_{1.15}$ spline.

by short edges improves closeness at the cost of non-uniformity. This non-uniformity challenges high-degree reproduction schemes.

6. Conclusion

We developed a framework for non-uniform interpolatory subdivision algorithms of prescribed smoothness, and presented examples of $2n$-point schemes of smoothness C^{n-1} for $n = 2, 3, 4$, as well as non-uniform interpolatory 6-point schemes with C^3 continuity, i.e. higher than expected. In particular, we found that the schemes based on lower degree interpolants are advantageous for highly non-uniform data. We discussed the trade-off between splines and subdivision by concrete examples, the simplicity of analysis and the quality of curvature plots. The final judgement, as to how practical non-uniform subdivision can be vis-a-vis the spline standard, is still out – we should not shy away from exploring all options.

Acknowledgments.

The work was supported in part by NSF Grant CCF-1117695. L. Romani helped us fully understand the constructions in [BCR11a, BCR11b] so that we could pinpoint the overlap and the differences to our constructions.

References

[ADS10] Ursula H. Augsdörfer, Neil A. Dodgson, and Malcolm A. Sabin. Variations on the four-point subdivision scheme. *Computer Aided Geometric Design*, 27(1):78–95, 2010.

[BCR11a] Carolina Beccari, Giulio Casciola, and Lucia Romani. Polynomial-based non-uniform interpolatory subdivision with features control. *Journal of Computational and Applied Mathematics*, 16(235):47544769, 2011.

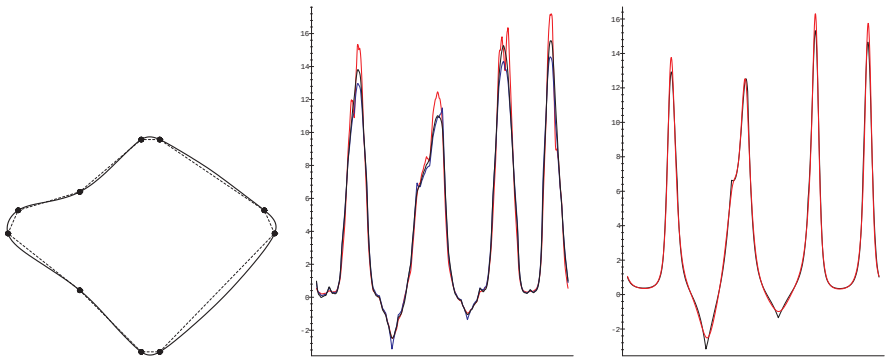

(a) Polygon and curve (b) curvatures (c) smoothing

Figure 7: (a) Input polygon and $\mathrm{cr}^2_{1.15}$ spline; (b) red: CR^2_w subdivision with $w = 0.0141$, black: $\mathrm{A}^{2,5:3}_{0.0141}$-subdivision. blue: $\mathrm{A}^{2,5:3}_{3/256}$ subdivision; (c) black: $\mathrm{cr}^2_{1.15}$ spline improved by red: the C^3 smoothed version accroding to Section 2.2.

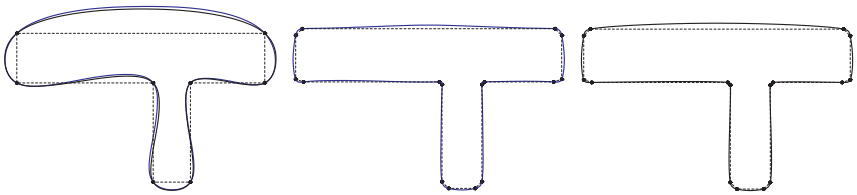

(a) T-shape & interpolants (b) $A^{2,5:3}_{3/256} = A^{2,5}$ (c) $\mathrm{CR}^2_{3/256}$

Figure 8: (a) Curves deviate from the T-shape. $A^{2,5:3}_{3/256} = A^{2,5}$ (blue) achieves quintic reproduction, while $\mathrm{CR}^2_{3/256}$ (black) achieves only quadratic reproduction. (b) $A^{2,5:3}_{3/256} = A^{2,5}$ shows unexpected wavyness when the corners are replaced by short line segments, compared to (c) $\mathrm{CR}^2_{3/256}$

[BCR11b] Carolina Vittoria Beccari, Giulio Casciola, and Lucia Romani. Non-uniform interpolatory curve subdivision with edge parameters built upon compactly supported fundamental splines. *BIT Numerical Mathematics*, 51(4):781–808, 2011.

[CR74] E. Catmull and R. Rom. A class of local interpolating splines. In R. Barnhill and R. Riesenfeld, editors, *Computer Aided Geometric Design*, pages 317–326. Academic Press, 1974.

[DFH04] Nira Dyn, Michael S. Floater, and Kai Hormann. A C^2 four-point subdivision scheme with fourth order accuracy and its extensions. In M. Daehlen, K. Morken, and L.L. Schumaker, editors, *Mathematical Methods for Curves and Surfaces, Tromsoe*, pages 145–156, 2004.

[DGS99] Ingrid Daubechies, Igor Guskov, and W. Sweldens. Regularity of irregular subdivision. *Constr. Approx.*, 15(3):381–426, 1999.

[DH] Nira Dyn and Kai Hormann. Geometric conditions for tangent continuity of interpolatory planar subdivision curves. *CAGD*. in press.

[DL02] Nira Dyn and David Levin. Subdivision schemes in geometric modelling. *Acta Numerica*, 11:73–144, 2002.

[DLG88] N. Dyn, D. Levin, and J. Gregory. A 4-point interpolatory subdivision scheme for curve design. *Computer Aided Geometric Design*, 4(4):257–268, 1988.

[DS78] D. Doo and M. Sabin. Behaviour of recursive division surfaces near extraordinary points. *Computer-Aided Design*, 10:356–360, September 1978.

[Dyn92] Nira Dyn. Subdivision schemes in computer-aided geometric design. In W Light, editor, *Advances in numerical analysis II*, pages 36–104. Oxford University Press, 1992.

[HMR09] Jochen Hechler, Bernhard Mößner, and Ulrich Reif. C^1-continuity of the generalized four-point scheme. *Linear Algebra and its Applications*, 430(11–12):3019–3029, June 2009.

[KLY07] Kwan Pyo Ko, Byung-Gook Lee, and Gang Joon Yoon. A study on the mask of interpolatory symmetric subdivision schemes. *Applied Mathematics and Computation*, 187(2):609–621, April 2007.

[Lan85] Serge Lang. *Complex Analysis*. Springer, New York, 2 edition, 1985.

[PR08] J. Peters and U. Reif. *Subdivision Surfaces*, volume 3 of *Geometry and Computing*. Springer-Verlag, New York, 2008.

[Rio92] Olivier Rioul. Simply regularity criteria for subdivision schemes. *SIAM J. Math. Anal.*, 23:1544–1576, 1992.

[Sab10] M. Sabin. *Analysis and Design of Univariate Subdivision Schemes*, volume 6 of *Geometry and Computing*. Springer-Verlag, New York, 2010.

[War95] J. Warren. Binary subdivision schemes for functions over irregular knot sequences. In Morten Dæhlen, Tom Lyche, and Larry L. Schumaker, editors, *Proceedings of the first Conference on Mathematical Methods for Curves and Surfaces (MMCS-94)*, pages 543–562, Nashville, USA, June 16–21 1995. Vanderbilt University Press.

[Wei90] A. Weissman. *A 6-point interpolatory subdivision scheme for curve design*. PhD thesis, Tel Aviv University, 1990.

[WW02] Joe Warren and Henrik Weimer. *Subdivision methods for geometric design: a constructive approach*. Computers. Morgan Kaufmann, 2002.